Tin-doped indium oxide thin films deposited by sol–gel dip-coating technique

K. Daoudi [*], B. Canut, M.G. Blanchin, C.S. Sandu, V.S. Teodorescu, J.A. Roger

Département de Physique des Matériaux, UMR CNRS 5586, Université Claude Bernard-Lyon 1, 43 boulevard du 11 Novembre 1918, 69622 Villeurbanne Cedex, France

Abstract

Indium tin oxide (ITO) thin films were prepared by the sol–gel dip-coating (SGDC) technique. The microstructure and electrical properties of ITO thin films crystallized using rapid thermal annealing (RTA) were compared with those of films prepared by classic thermal annealing (CTA). ITO thin films were successfully prepared by CTA at 500 °C for 30–60 min. At the same temperature of 500 °C and with a 6 min RTA treatment, the film exhibits electrical resistivity values close to the CTA ones. The crystalline structure of the ITO films was visualized by high-resolution transmission electron microscopy (HRTEM) and electron diffraction patterns compared with that of pure In_2O_3. The average grain size, measured from TEM micrographs, ranges from 5 to 20 nm. The process of film densification was also followed by Rutherford backscattering spectrometry (RBS).
© 2002 Elsevier Science B.V. All rights reserved.

Keywords: Indium tin oxide; Sol–gel; RTA; XTEM; RBS

1. Introduction

Indium tin oxide (ITO) is highly conductive and transparent to visible light. Based on these characteristics, ITO is an indispensable material for transparent electrodes in optoelectronic technologies. ITO thin films have been fabricated by various methods such as spray pyrolysis [1], electron beam evaporation [2], chemical vapour deposition [3], magnetron sputtering [4], radiofrequency sputtering [5], screen printing [6], pulsed-laser deposition [7] and more recently using the sol–gel technique [8–20]. When compared with other techniques, the sol–gel route presents some advantages such as possibility of depositing on complex-shaped substrates, easier control of the doping level, rather inexpensive starting materials and simple equipment. The optical and electrical properties of the sol–gel films are comparable with the best results reported so far. In order to obtain a sol–gel ITO film, after dipping or spinning, the wafers are dried then annealed in a conventional furnace at 500 °C for 1 h. These operations are repeated several times (up to 5) to obtain a sufficient thickness for practical applications [8]. Therefore, the preparation of one multi-layered sample with classic thermal annealing (CTA) holds out many hours. In this study, we present our first results on rapid thermal annealing (RTA) of sol–gel ITO thin films compared with the classical procedure. In previous works on the sol–gel Sb-doped SnO_2 [21–23], our research group has successfully used the antimony and tin chlorides as precursors. In the present experiments, ITO thin films were prepared using indium and tin chlorides as starting materials. Electrical behaviour and structural properties are presented and correlated with the preparation conditions of such obtained ITO thin films. A special attention is given to the comparison between the densification of the deposits.

2. Experimental details

Tin-doped indium oxide films were prepared using the sol–gel dip-coating (SGDC) procedure with a sol made from indium anhydrous trichloride ($InCl_3$) dissolved in acetylacetone and tin chloride ($SnCl_2 \cdot 2H_2O$) dissolved in ethanol. The two solutions were refluxed at 83 °C and then mixed. The 10 wt.% Sn concentration is fixed for all our experiments. Pyrex substrates were dipped in the starting solution and withdrawn at a rate of 8 cm min^{-1}. Two procedures for densification and crystallization are used.

---

[*] Corresponding author. Tel.: +33-4-72-44-81-87; fax: +33-4-72-43-15-92.

E-mail address: kais.daoudi@dpm.univ-lyon1.fr (K. Daoudi).

Fig. 1. RTA cycle.

Fig. 2. Evolution of the sheet resistance of the 10 wt.% Sn-doped ITO thin films as function of number of layers. The ITO thin films are annealed in air by CTA at 500 °C for 30 min (a), 60 min (b) and RTA (c).
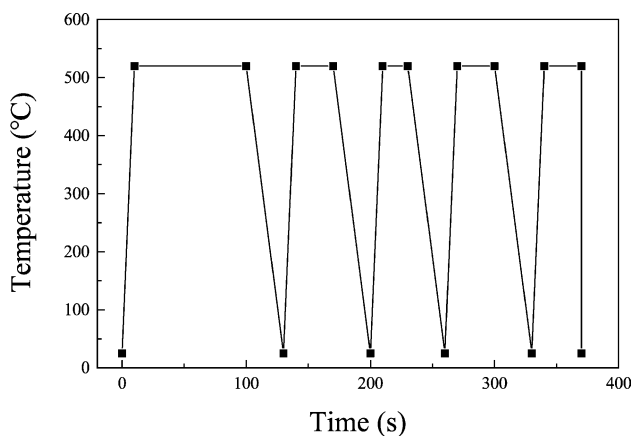
During the classical procedure, the wafers are dried in air for 30 min at 150 °C and then annealed in a conventional furnace in air at the temperature of 500 °C for 30–60 min. In the RTA procedure, the wafers are annealed in a JIPELEC Jetfirst 100 apparatus for 6 min. RTA cycle is presented in Fig. 1. In previous work on SnO_2/Sb, we have shown that such a RTA cycle gives the best electrical properties, certainly in reason of the alternance between heating and cooling phases [24].

Electrical performances were commonly measured with a 3 mm wide, four-probe apparatus. Cross-section transmission electron microscopy (XTEM) observations were performed using a high-resolution electron microscope Topcon 002B operated at 200 kV and capable of a 0.18 nm point-to-point resolution. The XTEM samples were prepared following the conventional cross-section method: mechanical cutting, gluing face-to-face with M bond, mechanical thinning and polishing and finally ion milling in a Gatan apparatus. Rutherford backscattering spectrometry (RBS) was performed with $^4He^+$ ions delivered by a 2 MeV Van de Graaff accelerator.

3. Results and discussions

3.1. Electrical properties

The variation of the sheet resistance (R_s) as a function of the number of stacked layers in the ITO films obtained by CTA and RTA is presented in Fig. 2. A strong decrease in R_s is observed for the two layers first deposit. This behaviour is linked to the starting of the crystallization and to the first steps of densification. It is clear that an increase in the classical annealing time from 30 to 60 min (Fig. 2a and b) leads to a decrease in the sheet resistance whatever the ITO thickness.

We evidence in Fig. 2c those ITO thin films fired by RTA procedure present systematically higher conductivity than those obtained by CTA procedure (Fig. 2a and b). For a
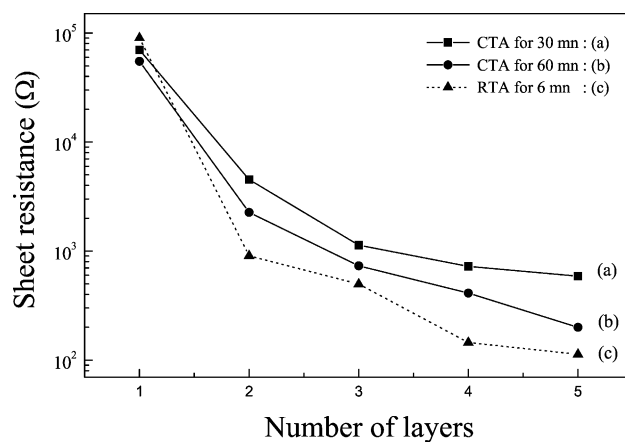
four-layered film, the resistivity is $4.9 \ 10^{-3} \ \Omega$ cm in the case of CTA and $3.6 \ 10^{-3} \ \Omega$ cm for RTA. Thus, a resistivity decrease of about 27% is observed. This improvement in conductivity for RTA films is probably due to a better percolation between grains (cf. Fig. 6).

3.2. Structural and morphological properties

3.2.1. Classical annealing

Fig. 3a shows a high-magnification, high-resolution transmission electron microscopy (HRTEM) image from a
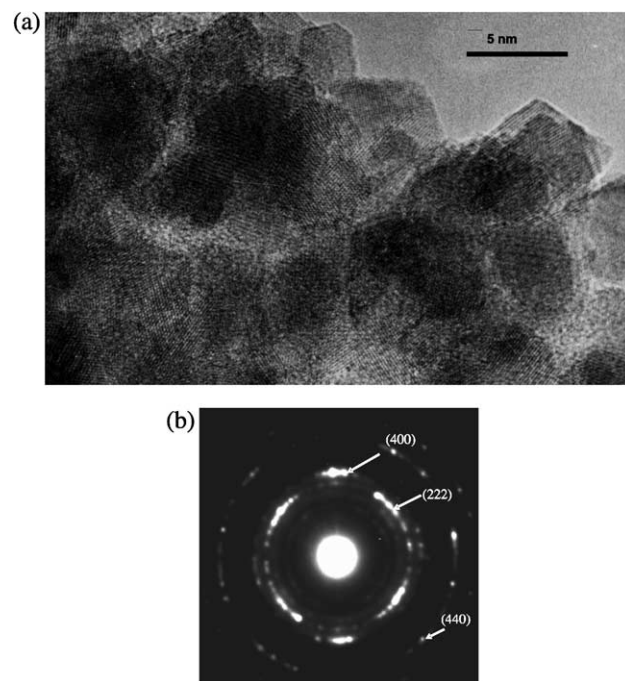

Fig. 3. HRTEM image (a) and diffraction pattern (b) of a two-layer deposit of an ITO thin film obtained by the CTA procedure in air at 500 °C for 1 h.
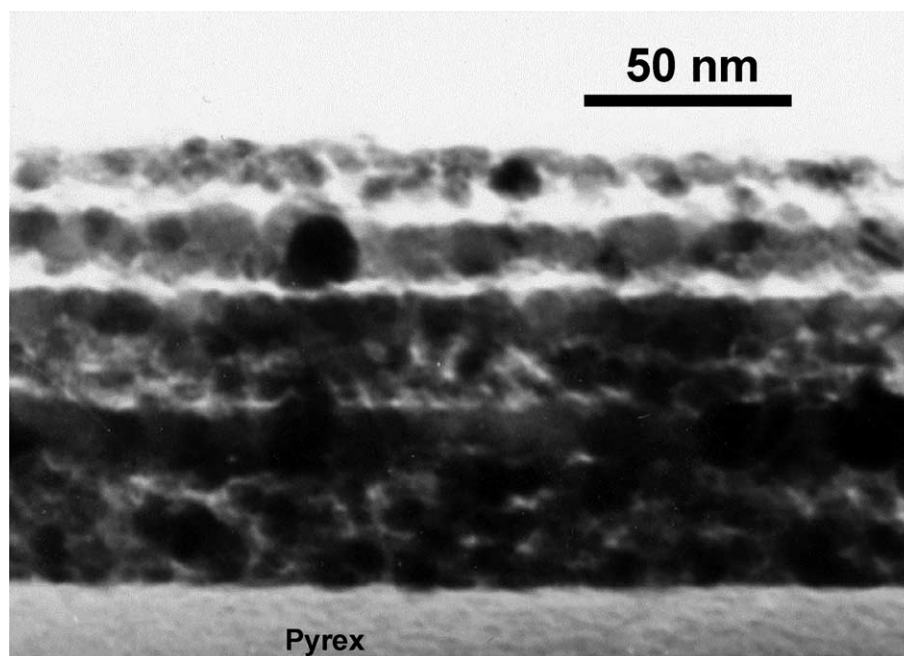
Fig. 4. XTEM image of a four-layer ITO (10 wt.% Sn) dried and annealed at 500 °C for 1 h after each deposited layer.

two-layered film obtained by the CTA procedure at 500 °C for 1 h. This film is polycrystalline, with the lattice fringes in the grains corresponding to main reflections of the indium oxide (In_2O_3) structure. The corresponding selected area electron diffraction (SAED) pattern (Fig. 3b) confirms that the grains have the In_2O_3 cubic structure.

Fig. 4 displays a cross-sectional view (XTEM) of an ITO film deposited on Pyrex substrate. This CTA film was obtained after four dip-coating cycles (each dried then densified at 500 °C for 1 h in air). The ITO film is about 125 nm thick, its structure is polycrystalline and the SAED reveals some texture. The four deposited layers can be distinguished because they are separated by a dense region forming a kind of "crust" (darker region in the image, parallel to the film surface). The grains in the film have a spheroidal morphology, with diameter ranging from 10 to 20 nm. The crystallites inside the "crust" are larger and their dimension can reach about 40 nm in the plane of the "crust".

The total film thickness for a given number of layers was measured on the corresponding cross-sections (XTEM images like in Fig. 4 for four layers). In Table 1, the variation of the total film thickness is reported as a function of the number of layers. The corresponding resistivity is directly deduced from the sheet resistance and thickness values. The layer thickness decreases by almost 33% from the first deposit to the second one and from the second to the third one. We do not observe the linear dependence of the film thickness on the dipping number reported in some other works [25]. The number of atoms per centimeter square, extracted from RBS data (Fig. 5), was correlated with the film thickness measured

from the XTEM images (Table 1). It is then possible to derive the number of atoms per volume unit (N) and the density (d) in each case (Table 1). We notice an increase in the density with the number of deposited layers. The SGDC ITO films can exhibit large density, i.e. 84% of bulk In_2O_3. We had already found in our research group a similar behaviour for SGDC SnO_2/Sb films: the increase of the film density with the number of layer is attributed to the filling the pores into the previous layer by the sol and to the growth of the "crust" regions [26].

3.2.2. Rapid thermal annealing

The XTEM image of a four-layered film of ITO obtained by RTA procedure is shown in Fig. 6. The film thickness is about 320 nm, a value higher than that of the film obtained by CTA procedure. This film evidences a polycrystalline structure showing the same reflections as indium oxide. In this film, the grain size distribution is

Table 1
CTA multilayered films

Number of layers	Annealing temperature (°C)	Film thickness (nm)	Resistivity (Ω cm)	Density (ITO/In_2O_3) (%)
1	500	50	2.7×10^{-1}	64.1
2		80	1.8×10^{-2}	65.5
3		105	7.7×10^{-3}	71.2
4		125	4.9×10^{-3}	77.3
5		145	2.9×10^{-3}	84.5

Evolution of thickness, electrical resistivity and atomic density as a function of the number of layers.
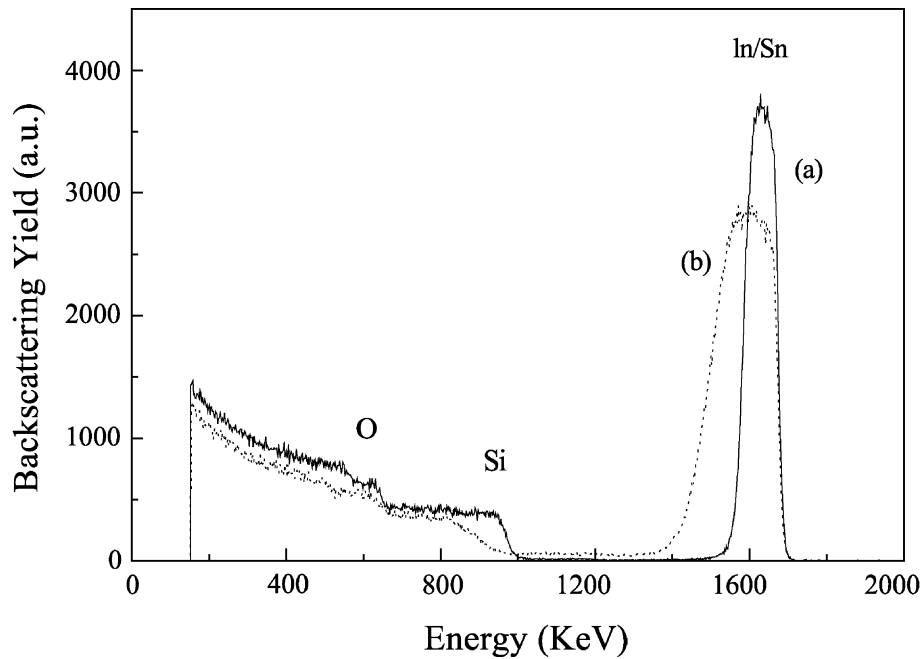
Fig. 5. RBS spectra of a four-layer ITO films crystallized by the CTA procedure (a) and RTA (b).

narrower (10–20 nm) than in CTA films. Moreover, in these ITO thin films, we cannot discern the four layers separated by the "crust" zone. This is probably linked to the short duration of densification and crystallization (6 min). The top part of the film close to the glue is texturised (cf. Fig. 6). Such a texture is evidenced by the asymmetry in the (In,Sn) peaks shown on the RBS spectrum (Fig. 5). Such textures in the last deposited layers cause an important decrease in the optical transmittance of the RTA films compared to CTA ones.

4. Conclusion

Indium tin oxide films have been successfully prepared by the dip-coating sol–gel process using tin and indium chlorides (low-cost precursors). Classical and rapid thermal annealings were used for densification and crystallization. The electrical properties were improved by the multilayer superposition. In the RTA procedure, the ITO films exhibit higher conductivity than those obtained by CTA. The XTEM investigations of the ITO multilayer deposits on
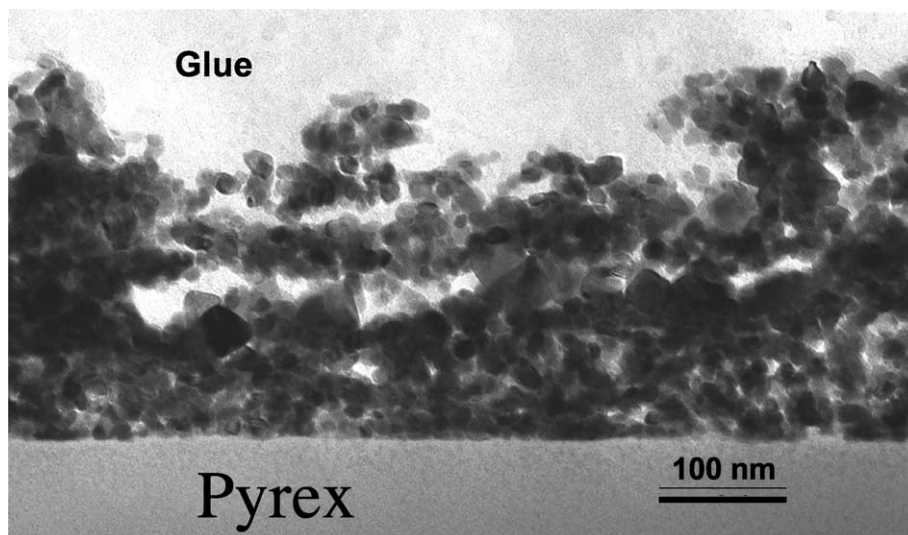

Fig. 6. XTEM image of a four-layer ITO (10 wt.% Sn) annealed by RTA at 500 °C for 6 min.

Pyrex substrates give key information on the way super-imposed layers crystallize.

Acknowledgements

References

[1] M. Mizuhashi, J. Non-Cryst. Solids 329 (1980) 38–39.

[2] Y. Shigesato, D.C. Paine, T.E. Hayens, Jpn. J. Appl. Phys. 32 (1993) L1352.

[3] J. Kane, H.P. Schweizer, Thin Solid Films 155 (1975) 29.

[4] M. Buchanan, J.B. Webb, D.F. Williams, Appl. Phys. Lett. 37 (1980) 213.

[5] K. Sreenivas, T.S. Rao, A. Mansinh, J. Appl. Phys. 57 (1985) 384.

[6] B. Bessaïs, N. Mliki, R. Bennaceur, Semicond. Sci. Technol. 8 (1993) 116J–121J.

[7] D.H. Lowndes, in: J.C. Miller, R.F. Haglund (Eds.), Laser Ablation and Desorption, Academic Press, San Diego, 1998, p. 551.

[8] R.B. Tahar, T. Ban, Y. Takahashi, J. Appl. Phys. 82 (1997) 865.

[9] N.J. Arfsten, J. Non-Cryst. Solids 63 (1984) 234.

[10] N.J. Arfsten, R. Kaufman, H. Dislich, Proceedings of the International Conference on Ultrastructure Processing of Ceramics, Glass and Composites, Wiley, New York, 1984, p. 189.

[11] H. Dislich, J. Non-Cryst. Solids 73 (1985) 599.

[12] T. Furusaki, K. Kodaira, in: P. Vincenzini (Ed.), High Performance Ceramic Films and Coating, Elsevier, Amsterdam, 1991, p. 241.

[13] K. Nishio, T. Sei, T. Tsuchiya, J. Mater. Sci. 31 (1996) 1761.

[14] D. Gallagher, F. Scanlan, R. Houriet, H.J. Mathieu, T.A. Ring, J. Mater. Res. 8 (1993) 3135.

[15] Y. Takahashi, S. Okada, R.B. Tahar, K. Nakano, T. Ban, Y. Ohya, J. Non-Cryst. Solids 218 (1993) 129.

[16] R.B. Tahar, T. Ban, Y. Ohya, Y. Takahashi, J. Appl. Phys. 83 (1998) 2139.

[17] T. Furusaki, K. Kodaira, M. Yamamoto, S. Shimada, T. Matsushita, Mater. Res. Bull. 21 (1986) 803.

[18] Y. Takahashi, H. Hayashi, Y.S. Okada, R.B. Tahar, K. Nakano, T. Ban, Y. Ohya, Mater. Res. Soc. Symp. Proc. 271 (1992) 401.

[19] D.J. Van Bommel, T.N.M. Bernards, W. Talen, Mater. Res. Symp. 346 (1994) 469.

[20] C. Goebbert, R. Nonninger, M.A. Aegerter, H. Schmidt, Thin Solid Films 351 (1999) 79.

[21] C. Terrier, J.P. Chatelon, R. Berjoan, J.A. Roger, Thin Solid Films 263 (1995) 37.

[22] C. Terrier, P. Chatelon, J.A. Roger, Thin Solid Films 295 (1997) 95.

[23] J.P. Chatelon, C. Terrier, J.A. Roger, Semicond. Sci. Technol. 14 (1999) 14.

[24] T. Boudiar, C.S. Sandu, B. Canut, M.G. Blanchin, V.S. Teodorescu, J.A. Roger, Proceeding of the 11th International Workshop on Glasses, Ceramics, Hybrids and Nanocomposites From Gel, Padova, Italy, September, 2001.

[25] M.J. Alam, D.C. Cameron, Thin Solid Films 377–378 (2000) 455–459.

[26] J.P. Chatelon, C. Terrier, J.A. Roger, Semicond. Sci. Technol. 4 (1999) 642–647.